MONOLITHICALLY INTEGRATED PIEZOMEMS SP2T SWITCH AND CONTOUR-MODE FILTERS

J.S. Pulskamp[1], D.C. Judy[1], R.G. Polcawich[1], R. Kaul[1], H. Chandrahalim[2], and S.A. Bhave[2]
[1]US Army Research Laboratory, Adelphi, MD, USA
[2]Cornell University, Ithaca, NY, USA

ABSTRACT

This paper provides the first experimental demonstration of monolithically integrated piezoelectric MEMS RF switches with contour mode filters. Lead zirconate titanate (PZT) thin films are utilized to enable both low-voltage switch operation and filter tunability. This research leverages previous work using PZT actuators for low-voltage, wide-band switches and PZT transduced silicon resonators. The two device technologies are combined using a hybrid fabrication process that combines the key components of each device fabrication into a single unified process using silicon-on-insulator (SOI) substrates. The voltage tunable and switchable PiezoMEMS filter array provides a drop-in solution for frequency-agile channel selectivity.

INTRODUCTION

RF MEMS has been a significant area of research for well over a decade due to the promise of improved performance and integration potential in commercial and military wireless communication and radar systems. RF MEMS switches have demonstrated superior performance in terms of insertion loss, isolation, power consumption, and linearity [1]. RF MEMS filter technologies can provide insertion loss, percent bandwidth, and rejection performance similar to off-chip crystal filters and surface acoustic wave (SAW) devices with the compact integration of multiple frequencies on the same chip [2-4]. The integration of these two technologies has long been a goal of researchers and will enable not only more compact and lower cost systems but previously unachievable signal processing functions [5].

A number of transduction approaches have been utilized for both MEMS switch and filter operation, including electrostatic, electromagnetic, electro-thermal, and piezoelectric. Piezoelectric and or ferroelectric transduction can provide superior electro-mechanical coupling and mechanical energy densities; metrics applicable to both switch and filter operation. Piezoelectric AlN is a popular filter material due to the high acoustic velocity, high mechanical quality factor, and the ease of post-CMOS integration [3]. AlN is generally the preferred material for direct piezoelectric effect transduction due to its favorable ratio of stress constant to dielectric constant.

Ferroelectric lead zirconate titanate (PZT) has an effective piezoelectric stress constant that is an order of magnitude larger than AlN and is generally the preferred material for indirect piezoelectric effect transduction [6]. Thin films of ferroelectric PZT also permit tuning of the piezoelectric coefficients, some elastic constants, permittivity, and hence the electro-mechanical coupling factor of the material with a modest DC bias. Low-voltage (<10 V) ohmic contact series switches with high isolation and good insertion loss characteristics up through 65 GHz have been demonstrated with surface micro-machined PZT MEMS [7]. Recently, PZT and PZT-on-SOI resonators and filters have shown low motional impedance (<50Ω) and good quality factor (2000-5100) with superior frequency tunability (5.1% and 0.2% respectively) [8]. The integration of PZT thin films with high mechanical quality factor single crystal silicon features allows a tradeoff between steep-walled narrow-bandwidth filters, low-*Q* wide-bandwidth filters, linearity and center frequency agility. Single pole dual throw (SP2T) PZT MEMS switches have also been previously demonstrated with better than 50 dB of isolation and less than 0.4 dB of insertion loss at 2 GHz [9]. Unlike AlN, integration of high quality piezoelectric PZT films with CMOS remains a challenge for MEMS applications because of the high process temperatures. However, PZT thin films with high quality ferroelectric properties have been successfully integrated with CMOS for ferroelectric random access memory (FeRAM) [10].

Recently, Sinha et. al. successfully co-fabricated aluminum nitride (AlN) switches and resonators and reported cascaded S-parameter data illustrating how a switchable resonator should function [11]. In this paper we report on the integration of a PZT RF MEMS single pole dual throw (SP2T) series switch with contour mode mechanically coupled PZT-on-SOI high quality factor filters and the first experimental demonstration of monolithically integrated piezoelectric MEMS RF switches and filters.

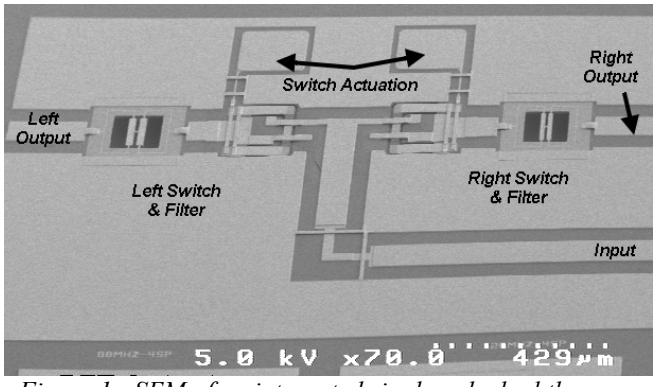

Figure 1: SEM of an integrated single pole dual throw PZT MEMS switch and two PZT contour mode filters.

DESIGN

Using a single pole dual throw (SP2T) architecture similar to that reported previously [8], two normally-open, ohmic contact, series switches were used to select between two contour mode mechanically coupled PZT-on- SOI high quality factor filters (see Fig. 1). As seen in Fig. 1, a conductive pad and contacts are located on the dielectric structure mechanically coupling the two cantilevered PZT unimorph actuators. The switch resides in the gaps of the co-planar waveguide (CPW)

transmission line. Unlike the cantilevered designs in [7,9], the RF gold air bridge contact structures above the switch contact pad were redesigned as clamped-clamped structures to mitigate deformation of these structures during and after fabrication. Two bias line air bridges located at the anchors of the actuators electrically connect the top and bottom electrodes of the two actuators. To enable switch biasing with a single trace, the top electrode bias line air bridge anchors to one of the CPW ground planes and the bottom electrode bias line air bridge anchors to a single bias line. The typical switch actuator composite stress states, composition, and thicknesses are designed to provide static negative curvature in the switch to dictate the preferred initial contact gap. The application of voltage to the top and bottom electrodes provides d_{31} mode bending actuation to the switch and raises the contact pad into contact with the two clamped-clamped RF gold air bridges. These devices were designed with analytical models, ANSYS, ADS Momentum, and HFSS. The Ohmic series switches and SP2T design are similar to the designs presented in [7,9].

The filter designs in this work are based on the work presented in [8]. The designs in this work feature significantly reduced parasitic shunt capacitances by reducing the top electrode contact area, not associated with the active transducer, through the use of air bridge structures available with the switch process steps (See Fig. 2b). The constituent resonators are fundamental width-extensional contour mode designs. Two of these resonators are coupled via an acoustic quarter-wave coupling spring (not simulated) to create a two-pole mechanically coupled filter (See Fig. 3). The filters presented in this paper were designed as 209MHz and 313MHz. The fundamental resonant frequency of the width extensional mode is given by:

$$f_o = \frac{n}{2W}\sqrt{\frac{Y_{eff}}{\rho_{eff}}} \tag{1}$$

where W is the width of the resonator, Y_{eff} and ρ_{eff} are elastic modulus and mass density of the composite resonator respectively, and n is the harmonic order. The bandwidth (BW) of such a mechanically-coupled filter is given by:

$$BW = \frac{f_o}{k_{ij}}\frac{k_s}{k_r} \tag{2}$$

where f_o is the resonant frequency, k_s and k_r are the spring stiffness of the coupling spring and resonator respectively and k_{ij} is the filter coefficient [12].

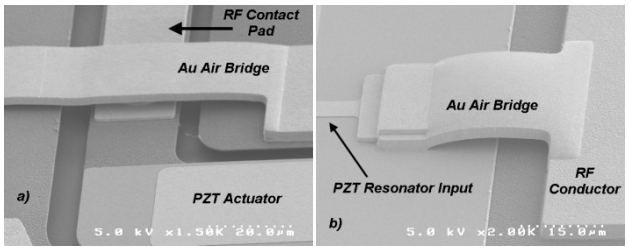

Figure 2: (a) SEM image of the air bridges used for switch operation and (b) reduced parasitics in the resonators.

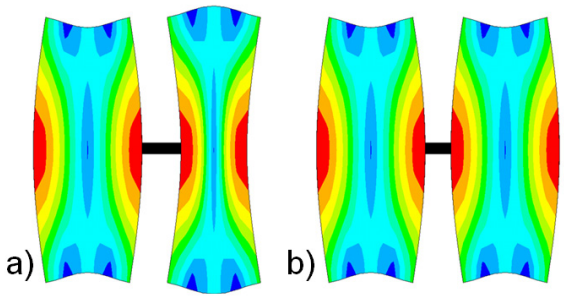

Figure 3: ANSYS mode shape of a fundamental width-extensional mode filter. (a) Anti-symmetric mode, (b)Symmetric mode

Relatively few modifications were required to integrate the two device types as most of the steps of the two individual processes were initially common. The substrate was chosen as SOI to accommodate the filters. The switch sacrificial layer features were altered to ensure proper release timing in the presence of the added passivation layer necessary to protect the device silicon features of the filter during the XeF_2 release and the release sequence was reversed to accommodate the integration.

FABRICATION

Device fabrication was done at the Specialty Electronic Materials and Sensors Cleanroom Facility, U.S. Army Research Laboratory, Adelphi, MD. The fabrication process for the monolithically integrated piezoelectric MEMS RF switches and filters utilized a silicon-on-insulator substrate with a 5 µm thick device layer with nominal resistivity of 30 Ohm-cm. A 5000 Å silicon dioxide thin-film was deposited by plasma-enhanced chemical vapor deposition (PECVD) and was followed by a sputtered Ti/Pt bottom electrode for the PZT deposition. The 5185 Å PZT thin films were prepared via a chemical solution derived deposition process modified from that outline in [13]. After the final PZT anneal, a 1050 Å platinum thin film was sputter deposited directly onto the PZT surface at 300ºC.

The switch actuator and filter drive and sense electrode were patterned with the argon ion-milling of the top platinum layer and was followed by an additional ion-milling of the PZT and bottom electrode features. A wet etch then opened up contact vias to the local bottom electrodes of the switches and filters. The switch structure was then further defined by patterning the silicon dioxide layer with a reactive ion etch to provide access to the silicon device layer for the eventual release etch. A titanium / gold bi-layer was then deposited with electron beam evaporation and patterned via liftoff to define the CPW transmission line, contact structures for the switch, and anchor features required for gold air bridges. A lift-off process was then used to pattern the switch contact material. The filters were defined using a single photomask by an ion-milling of the PZT and bottom electrode, an RIE of the silicon dioxide layer, a DRIE of the device silicon layer, followed by an RIE of the buried oxide layer. A photo-resist sacrificial layer was then patterned and cured and was followed by the deposition and lift-off of 2 µm gold air-bridge features necessary for both the switches and filters. A thick photo-resist layer

was then patterned to encase the silicon resonator features in resist and the buried oxide during release. The sidewalls of the switches and regions near the filters were not coated to permit a timed XeF_2 etch of the silicon device layer directly beneath the switch and the silicon handle layer beneath the filter. The release process reversed the typical release sequence utilized in [6], with the XeF_2 silicon etch preceding the oxygen plasma release of the gold air-bridge structures.

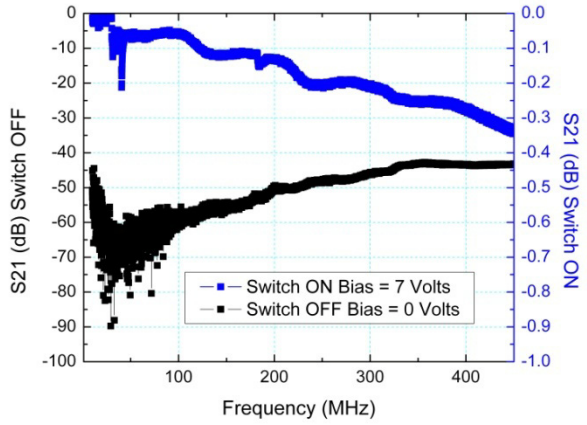

Figure 4: S_{21} data at 0 and 7 volts for the PZT MEMS switch co-fabricated with the PZT resonators.

EXPERIMENTAL RESULTS

All switch and filter measurements were completed with a network analyzer using a 50 Ohm termination. Individual switches exhibited isolation better than -40 dB from DC through 500 MHz (see Fig. 4). Switch actuation was achieved with the application of 7 volts resulting in an insertion loss less than -0.4 dB from DC to 500 MHz. Processing these devices on a relatively low resistivity SOI wafer resulted in the insertion loss being higher than the individual switches processed on silicon substrates with a resistivity greater than 10 kOhm-cm in previously reported research [6].

With both switches in the offstate (i.e. 0 volts applied), the output from both the left or right filters exhibit a flat S21 response with a magnitude of -60 dB (see Fig. 5a). This is somewhat surprising since a simple linear cascade of S parameters of the switch and resonator should show the filter response shifted down by the individual switch isolation as in [7]. Although this curiosity is still under investigation, we believe it is most likely due to current shunting around the open switch effectively reducing its isolation. The exclusion of air bridges at the SP2T junctions is a likely source of this reduced isolation.

As each switch was actuated at 7 volts, the associated filter response was detected at the relevant output port for each filter (see Fig. 5b and 5c). For both filters, an improvement in the insertion loss was observed with the application of a DC voltage applied to the RF signal through the bias tees of the network analyzer. The impedance tuning agrees with the previous observation of Chandrahalim et al. [7]. The filters exhibited out-of-band rejection of nearly -30 dB and a 50Ω terminated insertion loss of -17 dB and -24 dB (as measured from the minimum insertion loss) with the application of a 10 volt DC bias (see Fig. 5b and 5c). Similar filter responses were observed in the integrated (add 0.4 dB insertion loss) as in the standalone filters fabricated on the same wafer (See Fig 6). The similar performance between individual filters and filters integrated with SP2T switches suggest obtaining improved device performance is a matter of updating the filter design, which is currently in progress.

A series of time domain measurements were used to examine the switching and filter characteristics as a function of switch cycling. As shown in Fig. 7, the output response from the integrated switch and filter is ringing up with each switching pulse. It is unclear whether this is due to ring up of the filter or is influenced by the electrical time constant due to the switch contact resistance. Similar to previous PZT switches, the switch cycle lifetime is expected to last in excess of tens of millions of switch cycles and improve with more suitable contact materials, switch optimization, and integrated packaging.

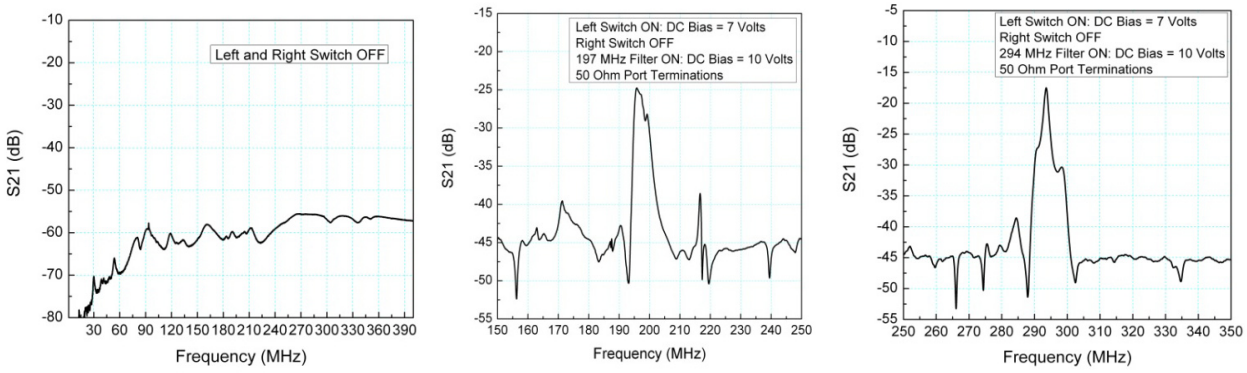

Figure 5: (a) S_{21} response for an integrated SP2T switch and filter with the switch in the off-state (0 V), (b) S_{21} response for the left switch and filter with the switch on (7 V) and with 10 V_{DC} applied to the filter, and (c) S_{21} response for the right switch and filter

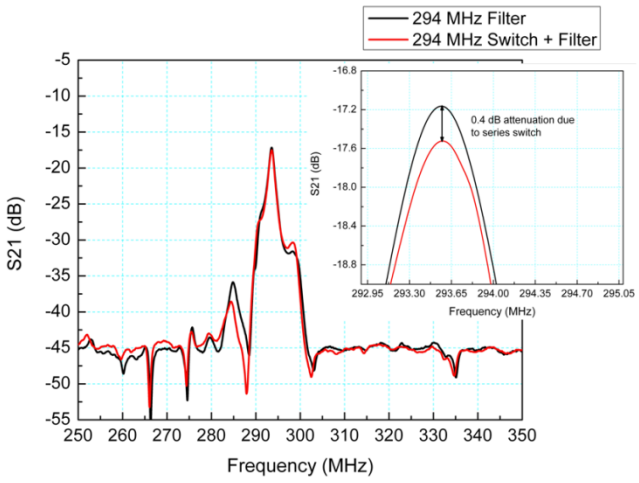

Figure 6: S_{21} response for a stand-alone PZT-on-SOI filter and an integrated PZT-on-SOI switch+filter with the DC bias at 10 volts for both devices (a). The switch increases insertion loss by 0.4dB (b).

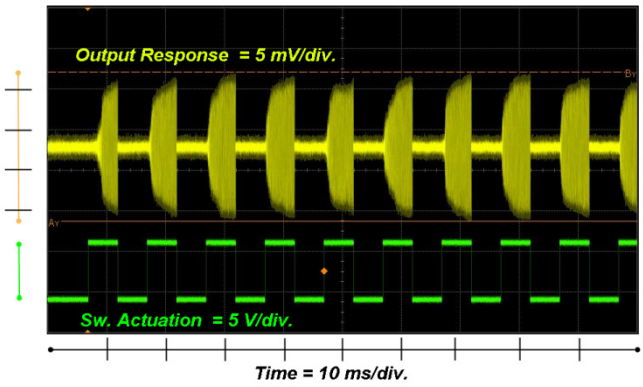

Figure 7: Time domain measurements of the switch+filter highlighting the 7V switching actuation pulses and the ring up response of the filter with the switch in the on state.

CONCLUSION

For the first time, piezoelectric MEMS RF switches and contour mode filters have been monolithically integrated and demonstrated as a switchable filter array. Lead zirconate titanate (PZT) thin films were utilized to enable both low voltage switch operation and filter tunability. On-going research is focusing on improving the loss performance of the filters, suppressing spurious modes, addressing switch lifetime, and incorporating wafer-level packaging. The low voltage switches and voltage tunable PiezoMEMS filter array provides a drop-in solution for frequency-agile channel selectivity.

ACKNOWLEGEMENTS

The authors wish to acknowledge the assistance and support of Joel Martin and Brian Power of General Technical Services and Richard Piekarz from the ARL for their hard work with device fabrication.

REFERENCES

[1] G. Rebeiz, *RF MEMS Theory, Design, and Technology*. Hoboken, NJ: Wiley, 2003.

[2] F. D. Bannon , J. R. Clark and C.T.-C. Nguyen "High-Q HF microelectromechanical filters," *IEEE J. Solid-State Circuits*, vol. 35, pp. 512, 2000.

[3] G. Piazza, et. al., "Single-Chip Multiple-Frequency AlN MEMS Filters Based on Contour-Mode Piezoelectric Resonators", *J. Microelectromech. Syst.*, vol. 16, pp. 319-328, 2007.

[4] H. Chandrahalim, D. Weinstein, L.F. Cheow, and S. A. Bhave, "Channel-select micromechanical filters using high-K dielectrically transduced MEMS resonators," MEMS'06, Istanbul, Turkey, pp. 894-897, 2006.

[5] Nguyen, C.T.-C, "Integrated Micromechanical Radio Front-Ends", VLSI Technology, Systems and Applications, 2008. VLSI-TSA 2008, pp. 3-4, 2008.

[6] P. Muralt, "PZT Thin Films for Microsensors and Actuators: Where Do We Stand?", IEEE Trans. Ultras. Ferro. Freq. Control, Vol. 47, pp. 903 – 915, 2000.

[7] R. G. Polcawich, et. al., "Surface micromachined microelectromechanical ohmic series switch using thin-film piezoelectric actuators," *IEEE Transactions Microwave Theory and Techniques*, Vol. 55, No. 12, pp. 2642 – 2654, 2007.

[8] H. Chandrahalim, et. al., "Influence of silicon on quality factor, motional impedance, and tuning range of PZT-transduced resonators," *2008 Solid State Sensor, Actuator and Microsystems Workshop*, Hilton Head Island, SC, pp. 360-363, 2008.

[9] D. J. Chung, et. al., "A SP2T and a SP4T Switch using Low Loss Piezoelectric MEMS," *IEEE MTT-S Microwave Symposium*, June 2008.

[10] Y. Arimoto and H. Ishiwara, "Current State of Ferroelectric Random-Access Memory", *MRS Bulletin, Nov. 2004, pp. 823-828.*

[11] N. Sinha, et. al., "Dual-beam actuation of piezoelectric AlN RF MEMS switches monolithically integrated with AlN contour-mode resonators," *2008 Solid State Sensor, Actuator and Microsystems Workshop*, Hilton Head Island, SC, pp. 22 - 25, 2008.

[12] A. I. Zverev, Handbook of Filter Synthesis. New York: Wiley, 1967.

[13] S. Dey, K. Budd, and D. Payne, "Thin-film ferroelectrics of PZT of sol-gel processing," TUFFC 35 (1) 1988, pp. 80-81.